Hydrodynamics of a Three-Phase Fluidized Bed Containing Low-Density Particles

Experiments were conducted to study the hydrodynamics of a gas-liquid-solid fluidized bed containing low-density particles. The density and size of the particles employed were comparable to those ordinarily encountered in fluidized-bed bioreactors for either wastewater treatment or fermentation. A dual resistivity probe and a conductivity probe were employed to study the axial holdup of gas and liquid phases and the bubble size distribution. The behavior of the axial holdup distribution for solid, gas, and liquid phases is reported. A mechanistic model, based on solids entrainment and deentrainment mechanisms by bubbles, is developed to describe the behavior of the axial solids holdup distribution. The model is shown to satisfactorily account for the experimental data.

Wen-Tzung Tang, Liang-Shih Fan
Department of Chemical Engineering
Ohio State University
Columbus, OH 43210

Introduction

The application of gas-liquid-solid fluidized-bed systems to biotechnological processes such as fermentation and aerobic wastewater treatment has gained considerable attention in recent years. In these three-phase biotechnological processes, biologically catalytic agents, either enzymes or living cells, are incorporated into the solid phase through immobilization techniques. Typically, enzymes or living cells are entrapped within natural or synthetic polymer gel particles or are attached to the surface of solid particles. These biologically active particles usually have an intermediate size from 500 μm to 3 mm, and a density very close to that of the liquid medium. For instance, alginate and agar gel particles, two widely used solid carriers in fermentation, have densities ranging from 1,020 to 1,050 kg/m^3. A sand particle with a diameter of 600 μm coated with a 200 μm biofilm has a density of about 1,300 kg/m^3.

One of the characteristics of a three-phase fluidized bed of low-density particles which most distinguishes it from that of high-density particles is the axial nonhomogeneity of the holdup (i.e., volume fraction) of the phases. Nonhomogeneity of the axial phase holdups is also common in slurry bubble columns. The behavior of slurry bubble columns has been extensively reported in the literature (Cova, 1966; Imafuku et al., 1968; Farkas and Leblond, 1969; Kato et al., 1972; Brian and Dyer, 1984; Ueyama et al., 1985; Smith and Ruether, 1985), whereas for three-phase fluidized beds, only a few studies have addressed the nonhomogeneity of the phase holdups. These studies have been primarily concerned with the freeboard behavior involving large ($d_p > 4.8$ mm) or heavy but small particles (Begovich and Watson, 1978; El-Temtamy and Epstein, 1980; Kato et al., 1985). Little has been reported regarding the in-bed phase holdup behavior involving low-density particles. The nonhomogeneity in the individual phase holdups affects the heat and mass transfer properties and hence the reactant conversion in a system where chemical reactions take place. Thus, understanding the phase holdup behavior is essential to the design, control, and optimum operation of a three-phase fluidized bed containing low-density particles.

In this study, the bubble and phase holdup characteristics of a three-phase fluidized bed containing low-density and intermediate size particles are investigated. An electrical conductivity probe is utilized for axial liquid holdup measurements. A mechanistic model is developed to account for axial solids holdup variation in the three-phase fluidized bed.

Phase Holdup Measurements

In a three-phase fluidized bed of heavy particles, the solids bed height can be determined from the interception of the two straight lines tangent to the pressure profiles in the two-phase and three-phase regions (El-Temtamy and Epstein, 1980). In preliminary experiments of this study, the pressure profile of a fluidized bed of polystyrene particles exhibiting a nonuniform axial distribution of solids appeared very close to a single straight line through two-phase and three-phase regions. Thus the pressure gradient method can no longer be used. Information about the individual phase holdup distributions is therefore needed to characterize such systems.

Correspondence concerning this paper should be addressed to L.-S. Fan.

Evaluation of the axial holdups of the gas, liquid, and solid phases in a three-phase fluidized bed is usually performed by determining one axial phase holdup and obtaining the other two by solving Eqs. 1 and 2 simultaneously:

$$\epsilon_S + \epsilon_L + \epsilon_G = 1 \tag{1}$$

$$-\frac{dP}{dz} = (\rho_S\epsilon_S + \rho_L\epsilon_L + \rho_G\epsilon_G)g + \left(\rho_S\epsilon_S u_S \frac{du_S}{dz} + \rho_L\epsilon_L u_L \frac{du_L}{dz} + \rho_G\epsilon_G u_b \frac{du_b}{dz}\right) - F_w \tag{2}$$

where ϵ_S, ϵ_L, and ϵ_G are the axial holdup (i.e., volume fraction) of solids, liquid, and gas, respectively. These equations are obtained based on the one-dimensional steady-state mass and momentum balances. Equation 2 assumes negligible interaction between gas and solids, which is valid for the light, wettable particles used in this study. The second term on the righthand side of Eq. 2 is the average convective flux of momentum arising from the axial nonuniformity of phase holdups. In a fluidized bed, there is no net flow of solids through the system. At steady state, the average momentum flux of solids, $\rho_S\epsilon_S u_S(du_s/dz)$, at any axial position is therefore zero. The entire convective momentum term vanishes when the phase holdups are invariant with respect to axial position. F_w accounts for the frictional loss due to fluid-wall interactions. Later, it will be shown experimentally that the convective and frictional terms of Eq. 2 are negligible for three-phase fluidized beds of low-density particles. The simplified equation thus becomes:

$$-\frac{dP}{dz} = (\rho_S\epsilon_S + \rho_L\epsilon_L + \rho_G\epsilon_G)g \tag{3}$$

In order to solve for the holdup of each of the three phases based on Eqs. 1 and 3, an additional relationship is required. This relationship is usually obtained by direct measurement of the axial holdup of one individual phase. However, direct measurement of the gas holdup using, for example, an electrical resistivity probe (Matsuura and Fan, 1984), does not yield reasonable values of the solids and liquid holdups after solving Eqs. 1 and 3, due to the very small density difference between the particles and liquid. Thus, it is necessary to measure directly either solids or liquid holdup. Direct sampling of solids has been extensively used in slurry bubble columns with particles smaller than 200 μm to measure the axial solids holdup. For larger, fluidized particles, however, this method requires laborious calibration due to significant particle inertia effects (Page and Harrison, 1974).

In this study, the axial liquid holdup was directly measured using an electrical conductivity method. The conductivity method was utilized because the relationship between the dispersed phase holdup and the effective electrical conductivity of a heterogeneous system has been subjected to rigorous theoretical treatments. In addition, the thermal conductivity, dielectric constant, and magnetic permeability of a heterogeneous material can be formulated in a way precisely analogous to that used in the treatment of the electrical conductivity. Consequently, the theoretical and experimental results derived for any of the above phenomena can be readily applied to others (Turner, 1976). These theoretical treatments lay the foundation for wide applicability of the conductivity method in measuring the volume fraction of either the dispersed or the continuous phase in a mixture. Tedious calibration can thus be minimized.

Maxwell (1881) provided the first theoretical analysis relating the effective conductivity, k, to the dispersed phase holdup, ϵ_d, of a heterogeneous two-phase system containing a dilute and randomly, homogeneously distributed spherical dispersed phase. The equation is expressed as:

$$\frac{k}{k_c} = \frac{1 + 2\beta\epsilon_d}{1 - \beta\epsilon_d} \tag{4}$$

and β is given by:

$$\beta = \frac{k_d - k_c}{k_d + 2k_c} = \frac{\alpha - 1}{\alpha + 2}, \alpha = \frac{k_d}{k_c} \tag{5}$$

where k_c and k_d are the conductivity of the pure continuous and dispersed phases, respectively.

Bruggeman (1935) considered the effective conductivity of a heterogeneous system containing spheres of a wide size distribution. For nearly nonconductive dispersed spheres ($\alpha \approx 0$), his equation simplifies to:

$$\frac{k}{k_c} = (1 - \epsilon_d)^{3/2} \tag{6}$$

Buyevich (1974) formulated an approximate theory to evaluate the effective thermal conductivity of a composite material composed of randomly distributed spherical granules with variable sizes and thermal conductivities. He viewed the dispersed particles as being surrounded by the continuous phase, of which the thermal potential is disturbed by the presence of the particles. The mutual exclusiveness of the spheres in space was taken into account. In addition, distribution of particle size was considered. The disturbance due to the presence of the dispersed particles was approximated by the point dipoles superimposed on the unperturbed potential field of the continuous phase. The equations thus obtained are lengthy, but can be simplified as follows for $\alpha \ll 1$:

$$\frac{k}{k_c} = \frac{24 - 17\epsilon_d}{24 + 19\epsilon_d} \tag{7}$$

It is seen that the conductivity mainly depends on volume fraction of dispersed phase but not on the particle size variation.

In addition to theoretical derivations, empirical expressions have also been proposed (Begovich and Watson, 1978; Kato, et al., 1981) with the form:

$$k/k_c = (1 - \epsilon_d)^n \quad \text{for } \alpha \ll 1 \tag{8}$$

where n is commonly in the range from 1.0 to 1.5.

Particle shape affects the effective conductivity-particle volume fraction relationship. Such an effect has been extensively discussed by Meredith and Tobias (1962).

The above theoretical equations have all been found applicable for phase holdup measurements in liquid-solid systems, depending on the particle size and shape, and perhaps the probe dimension and design. Turner (1976) reported that the Maxwell

equation held well even at high ϵ_d (up to packed bed values) and low α (<10) for fluidized beds of uniform, spherical particles smaller than 1 mm dia. The Bruggeman equation, on the other hand, was found to predict closely the effective conductivity of a well-mixed liquid-solid system containing spherical particles with a diameter from 0.063 to 6.25 mm (De La Rue and Tobias, 1959) and of a fluidized bed of 0.6 mm sand particles of irregular shape (Nasr-El-Din et al., 1987).

The conductivity probe method was used to measure axial liquid phase holdup in three-phase fluidized beds of large ($d_p > 4.8$ mm) particles (Begovich and Watson, 1978) and of small to intermediate size ($0.42 < d_p < 2.2$ mm) glass beads (Kato et al., 1981). In both cases, the probe was calibrated based on the liquid-solid system, and Eq. 10 with n equal to 1.0 and 1.2, respectively, was found to be applicable. No calibrations were performed in the three-phase system by Kato et al. (1981) and a poor agreement in liquid phase holdup calibration was presented by Begovich and Watson (1978). In the present study, the probe is calibrated in gas-liquid, liquid-solid, and three-phase systems and the respective literature equations are tested for their applicability.

Analysis

The axial solids distribution in a three-phase fluidized bed results from complex solids entrainment and deentrainment mechanisms due to the dynamics of bubble motion. During the course of a bubble's rise in a three-phase fluidized bed, liquid and solids are continually entrained into the wake that follows the bubbles. Bubbles also translate both liquid and solids near bubble roof upward, an effect known as drift. The wake and drift effects are lumped together and are defined here as being contributed by the bubble-engagement phase. This region is distinct from the particulate fluidization region and is assumed to rise at the same velocity as the bubbles. The solids in the engagement region are discharged by continuous settling due to gravity and by periodic wake shedding from the engagement region. The detailed mechanisms of solids entrainment and deentrainment have recently been explored by Tsuchiya and Fan (1988).

There are a few mathematical models proposed for describing the axial solids distribution in a slurry bubble column or in the freeboard region of a three-phase fluidized bed. The most widely used model is the so-called dispersion-sedimentation model (Cova, 1966, Imafuku, et al., 1968):

$$E_z \frac{dC_s}{dz} + U_p C_s = 0 \quad \text{for zero solids throughflow} \qquad (9)$$

where E_z is the solids axial dispersion coefficient and U_p is the so-called solids settling velocity. This model, however, does not consider pertinent physical mechanisms. Consequently, the physical meaning of the U_p term is dubious and has been subjected to inconsistent interpretations by various investigators. For instance, U_p was regarded as the single particle terminal falling velocity (Cova, 1966; Kojima and Asano, 1981), the hindered settling velocity of a particle swarm (Imafuku et al., 1968; Ueyama et al., 1985), or, with E_z, as an adjustable parameter obtained by fitting the model to experimental data (Kato et al., 1972; Smith and Ruether, 1984).

Other models formulated based on simplified mechanisms have also been proposed. El-Temtamy and Epstein (1980) modeled the deentrainment and entrainment of solids in the freeboard of a three-phase fluidized bed as a stagewise partition process. The size of each stage corresponded to the distance traveled by a bubble during which a wake shedding occurred. Dayan and Zalmanovich (1982) modeled the solids dispersion of a slurry bubble column system for bubbles with a closed turbulent wake; Turi and Ng (1986) formulated a model for solids entrainment merely by the upward drift of small spherical bubbles in a slurry bubble column.

In the present model, the three-phase fluidized bed is regarded as consisting of three distinct regions: the bubbles, the bubble-engagement region, and the liquid-solid particulate fluidization region. The present system is mostly operated under the dispersed bubble regime. The interaction among bubbles and among the bubble-engagement regions associated with each bubble is assumed to be negligible. A mass balance around the engagement region associated with each bubble in the three-phase fluidized bed yields:

$$V_R \frac{\epsilon_e}{N_b} \frac{d\epsilon_{Se}}{dt} = v_e A_e \epsilon_{Sf} - v_d A_d \epsilon_{Se} \qquad (10)$$

where V_R is the total volume of the three-phase fluidized bed; N_b is the total number of bubbles in the system; ϵ_e is the overall holdup of the bubble-engagement phase and is related to the overall gas holdup, $\bar{\epsilon}_G$, by:

$$\epsilon_e / \bar{\epsilon}_G = \eta \qquad (11)$$

The first term on the righthand side of Eq. 10 accounts for the rate of solids entrainment into the engagement region. It is postulated proportional to the solids concentration in the particulate fluidization phase ϵ_{Sf}, and the average velocity of solids relative to the bubble rise velocity v_e, across the effective area A_e. The second term is the rate of solids discharge from the engagement phase, accounting for solids discharge by settling and periodic wake shedding. For simplicity, the solids discharge is approximated as a continuous discharge process with a rate proportional to the solids concentration in the engagement region ϵ_{Se}, and an average solids discharge velocity v_d, which flows across an effective area A_d. The entrainment of solids into the wake region occurs for solids originally on top of the bubble and which have a trajectory lying within the liquid shear layer near the lateral edge of the bubble (Tsuchiya and Fan, 1988); the engagement of solids with the drift depends on the flow field of liquid surrounding the bubbles. The phenomena are very complex and are very difficult to quantify. Therefore, the boundary of solids entrainment and deentrainment areas can not be clearly defined. As will be shown later, direct evaluation of these areas is not necessary for the present analysis. Under the condition of no interaction among the engagement regions associated with each bubble, the axial position of the bubble can be related to the time coordinate by:

$$u_b dt = dz \qquad (12)$$

At steady state, the upward flow of solids in the engagement phase must be balanced by a net downward flow of solids in the particulate fluidization phase. A mass balance around a differ-

ential section of the bed gives:

$$u_b\epsilon_e \frac{d\epsilon_{Se}}{dz} = \epsilon_f \frac{d(v_p\epsilon_{Sf})}{dz} \tag{13}$$

Integrating Eq. 13 from z to H, the exit of the bed, with the boundary condition:

$$\epsilon_{Se} = \epsilon_{Sf} = 0 \quad \text{or} \quad \frac{d\epsilon_{Se}}{dz} = \frac{d(v_p\epsilon_{Sf})}{dz} = 0 \quad \text{at } z = H \tag{14}$$

yields:

$$u_b\epsilon_e\epsilon_{Se} = v_p\epsilon_f\epsilon_{Sf} \quad \text{at any } z \tag{15}$$

where v_p is the absolute magnitude of the linear net downward velocity of solids in the particulate fluidization region. Combining Eqs. 10, 12, and 15 gives:

$$V_R u_b \frac{\epsilon_e}{N_b}\frac{d\epsilon_{Se}}{dz} = \left(\frac{v_e A_e}{v_p} - \frac{v_d A_d \epsilon_f}{u_b\epsilon_e}\right) v_p\epsilon_{Sf} \tag{16}$$

Consider that the solids concentration in the engagement phase relative to that in the particulate fluidization phase, x, that is,

$$\epsilon_{Se}/\epsilon_{Sf} = x \tag{17}$$

is only a weak function of the axial position, and may be assumed constant with respect to the axial position (El-Temtamy and Epstein, 1980). Substituting Eq. 17 into Eq. 16 and rearranging gives:

$$\frac{V_R u_b \epsilon_e x}{N_b[v_e A_e/v_p - v_d A_d \epsilon_f/(u_b\epsilon_e)]}\frac{d\epsilon_{Sf}}{dz} = v_p\epsilon_{Sf} \tag{18}$$

Define E_z as:

$$E_z = -\frac{V_R u_b x \epsilon_e}{N_b[v_e A_e/v_p - v_d A_d \epsilon_f/(u_b\epsilon_e)]} \tag{19}$$

The E_z term thus represents the solids dispersion due to solids upward flow in the engagement region and solids entrainment and deentrainment effects. It may be a weak function of z, but can be approximated as constant. The solids concentrations, ϵ_{Sf} and ϵ_S, are interrelated by mass balance:

$$\epsilon_{Sf} = \frac{\epsilon_S}{x\epsilon_e + \epsilon_f} = \frac{\epsilon_S}{x\eta\epsilon_G + (1 - \epsilon_G - \eta\epsilon_G)} \tag{20}$$

Using Eq. 20 and with x and η assumed constant with respect to axial position (see Figure 3 for justification of the constant ϵ_G assumption), Eq. 18 can readily be converted to:

$$E_z \frac{d\epsilon_S}{dz} + v_p\epsilon_S = 0 \tag{21}$$

The resultant proposed model takes the same form as the dispersion-sedimentation model, Eq. 9, with E_z accounting for the solids upward dispersion, v_p representing the solids settling in the particulate fluidization region, and ϵ_S related to C_S by:

$$C_S(1 - \epsilon_G) = \rho_S\epsilon_S \tag{22}$$

The velocity of solids relative to the liquid, v_s, is given as:

$$v_s = v_p + v_{Lf} \tag{23}$$

where v_{Lf} is the linear liquid velocity in the particulate fluidization phase, and the velocities are expressed in terms of absolute scalar magnitudes. Substituting Eq. 23 into Eq. 21, one obtains:

$$E_z \frac{d\epsilon_S}{dz} + (v_s - v_{Lf})\epsilon_S = 0 \tag{24}$$

With the assumption that the engagement region rises at the same velocity as the bubbles, the linear liquid velocity in the particulate fluidization region is given by the material balance:

$$v_{Lf} = \frac{U_L - (U_G/\epsilon_G)(1 - \epsilon_{Se})\epsilon_e}{(1 - \epsilon_{Sf})(1 - \epsilon_G - \epsilon_e)} = \frac{U_L - (U_G/\epsilon_G)(1 - x\epsilon_{Sf})\eta\epsilon_G}{(1 - \epsilon_{Sf})(1 - \epsilon_G - \eta\epsilon_G)} \tag{25}$$

Assuming that the particulate fluidization region is not influenced by bubbles, v_s can be related to the liquid holdup in the particulate fluidization phase, ϵ_{Lf}, by any appropriate equation for particulate fluidization, for example, the Richardson-Zaki expression:

$$v_s = U_{t0}(\epsilon_{Lf})^{n-1} = U_{t0}(1 - \epsilon_{Sf})^{n-1} \tag{26}$$

where U_{t0} is the terminal falling velocity of a single particle in an infinite liquid medium, ϵ_{Sf} is given by Eq. 20, and n is found using the correlation equations given by Richardson and Zaki (1954).

The solids distribution in the entrance region of the bed is complicated by the jetting effects of gas and liquid flows. The proposed model may not be practically applicable to this region. This is evidenced in some operating conditions where a constant solids concentration with respect to the axial distance is observed for this region. The boundary condition can therefore be expressed by:

$$\epsilon_S = \epsilon_{S0} \quad \text{for} \quad z \le L_m \tag{27}$$

where ϵ_{S0} is the experimental solids holdup within the constant solids holdup height, L_m. To obtain the axial solids distribution, Eqs. 24 to 26 and Eq. 27 are solved simultaneously. The parameters E_z, η, x, and L_m cannot be directly predicted due to the complexity of the system. The numerical values of these parameters are obtained by parametric fitting of Eqs. 24–26 to the experimental axial solids concentration profile. A nonlinear pattern search algorithm is employed for the parametric fitting, which gives a minimum value of the sum of squares of the error under the constraints that: $0.8 \le x \le 1.3$; $0 \le E_z$; $0 \le \eta \le 10$; and that mass conservation:

$$\int_0^H \epsilon_S(z)\, dz = \frac{W}{\rho_S A} \tag{28}$$

is maintained. W is the total solids weight. The constraint on x is imposed based on recent results obtained by Kitano and Fan (1988). Equation 24 cannot be explicitly integrated. Its solution is obtained numerically using the fourth-order Runge-Kutta method.

Experimental Method

A diagram of the three-phase fluidized bed apparatus used in this study is shown in Figure 1. The main column is a transparent acrylic cylinder of 7.65×10^{-2} m ID and 1.285 m length. A cylindrical stainless steel screen with a nominal pore size of 0.75 mm is placed at the top of the column to prevent the elutriation of particles at high gas and/or liquid flow conditions. Air and liquid are introduced through a two-phase distributor where the two phases are premixed in a packed-bed portion, then redistributed into the bed through a PMMA (poly methylmethacrylate) porous plate with a nominal pore size of 30 μm. The liquid temperature for all the experimental runs was maintained at 24 ± 0.5°C. Table 1 summarizes the properties of particles used in this study.

The axial liquid holdup (averaged over the cross section at any axial position) is measured by an electrical conductivity probe of a design similar to that used by Begovich and Watson (1978). The probe consists of two platinized platinum electrodes. The electrodes are 0.02 m long and 0.01 m wide, and are attached to two pieces of 3.0 mm stainless steel tube. The two tubes are fixed 180° apart on an elliptic ring support 0.3 m above the electrodes. The elliptic ring is made from 1.2 mm dia. stainless steel tubing; its principal axis is equal to the inside diameter of the column. Insulated wires are passed through the stainless steel tubing and connected to a conductivity meter. The output signal of the conductivity meter is interfaced with an IBM personal computer. At least 1,000 data points were sampled and averaged for each axial holdup measurement.

A dual electrical resistivity probe (Matsuura and Fan, 1984) was used to determine the bubble size distribution. This probe

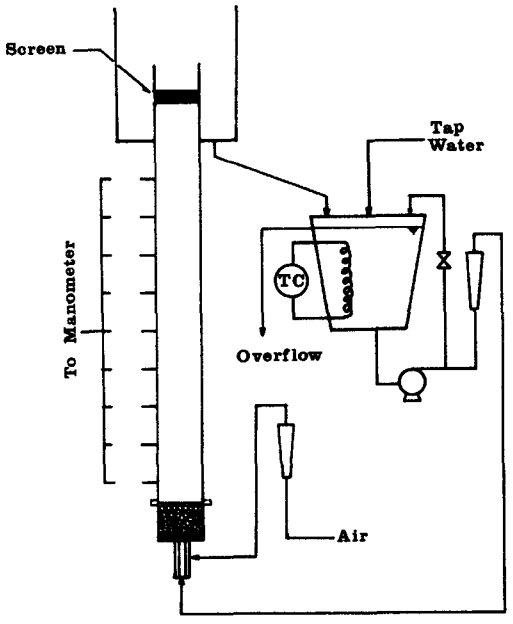

Figure 1. Three-phase fluidized bed.
TC, temperature controller

Table 1. Physical Properties of Particles

Particles	d_p μm	ρ_S kg/m^3	U_{t0} m/s	U_{mf} m/s
Polystyrene (PS2000)	2,000	1,050	0.026	0.0011
Acetate (AT1000)	1,000	1,300	0.048	0.0017
Acrylic (AR1500)	1,500	1,180	0.055	0.0029
Nylon (NY6350)	6,350	1,150	—	—

was also used to measure the axial gas holdup. The overall gas holdup of the present system was determined by the quick-closing-valve technique, that is, simultaneously shutting off the gas and liquid flows. The use of inclined manometers was required to obtain accurate pressure data due to the small density difference between the particles and the liquid phase.

Results and Discussion

Probe calibration

When applying the conductivity method for phase holdup measurements, it is essential to identify a valid equation that applies to both liquid-solid and liquid-gas systems such that the method can be consistently extended to three-phase systems. All experimental runs in this study used tap water as the liquid phase. Figure 2 summarizes the calibration results for various spherical particles in a liquid-solid fluidized bed. The figure shows that the measured effective conductivity-solids holdup relationship of acetate 1.0 mm particles follows the Bruggeman equation very closely, while the Buyevich equation, Eq. 7, best fits all the results with particles larger than 1.0 mm—acrylic, polystyrene, and nylon particles—for a solids holdup smaller than 0.4. The necessary condition, namely $\alpha \ll 1$, for applying Eq. 7 is met in the present tap water-solids systems, as exemplified in Figure 2 from the calibration result for polystyrene particles in a 1.0 M NaCl solution. The Buyevich equation also predicts the data of glass beads of 1.5, 2.8, and 5.5 mm from Figure 11 of Nasr-El-Din et al. (1987). Figure 2 also shows the calibration results for the gas holdup in a gas-liquid system at various gas flow rates. It is seen that both the Maxwell and Bruggeman equations are applicable for a gas holdup up to approximately 0.13, and the Buyevich equation accurately describes the effec-

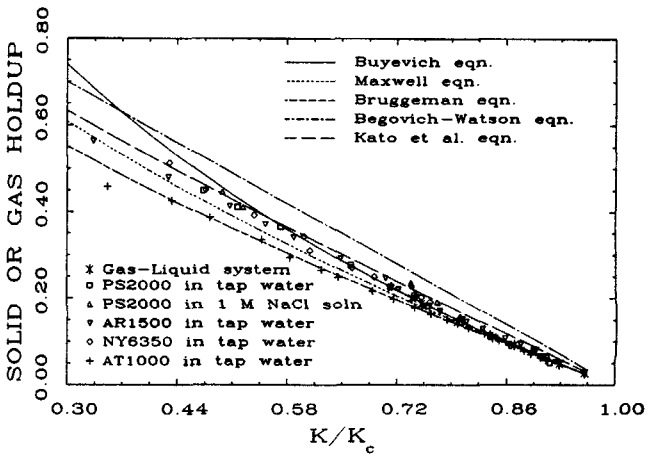

Figure 2. Probe calibration for liquid-solid fluidized beds and for a gas-liquid system.

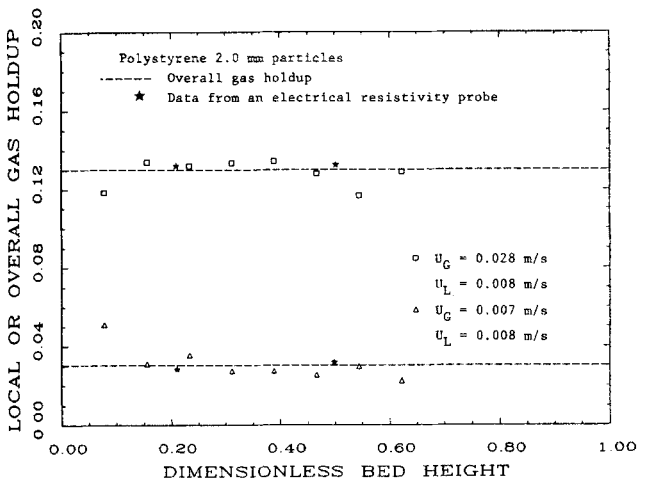

Figure 3. Axial gas holdup in a three-phase fluidized bed of polystyrene particles.
□△ Calculated using Eqs. 1 and 3

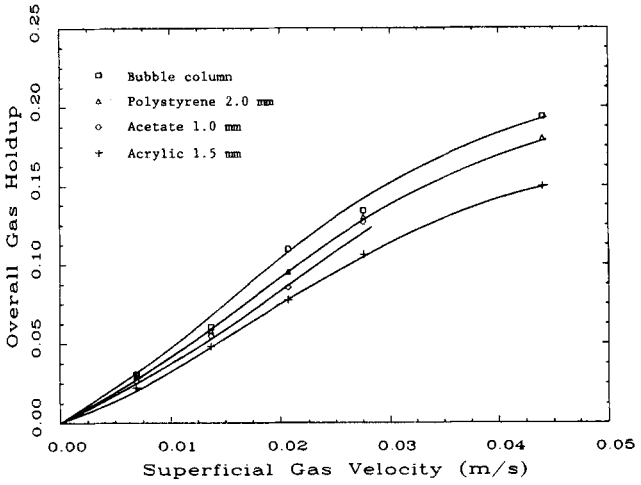

Figure 4. Average gas holdup in a bubble column and in three-phase fluidized beds of listed particles.
U_L = 0.008 m/s

tive conductivity-gas volume fraction relationship up to a gas holdup of 0.2. Note that the empirical equations proposed by Begovich and Watson (1978) and Kato et al. (1981) do not give satisfactory predictions for both gas-liquid and liquid-solid systems.

The applicability of the Buyevich equation to both liquid-solid and gas-liquid systems provides a basis for its use for gas-liquid-solid systems with spherical particles of sizes greater than 1.5 mm. For acetate 1.0 mm particles, the gas holdup obtained in this study was less than 0.14. The Bruggeman equation can thus be applied to the three-phase system of acetate particles. The applicability of the conductivity method and the equations described above are further verified by examining the sum of the experimentally measured overall gas holdup and overall solids holdup, and the overall liquid holdup integrated from the axial liquid holdup determined by the conductivity probe. The sums for all experimental runs are found to be 1 ± 0.003.

Figure 3 shows a comparison of the axial gas holdup determined from the electrical resistivity probe, the overall gas holdup, and the calculated axial gas holdup based on Eqs. 1 and 3 with measured liquid holdup and axial pressure profile. The close agreement in these comparisons reveals that:

1. The contribution of both the wall friction and the convective flux resulting from nonuniform phase holdups distribution in Eq. 2 can be neglected without introducing any significant error.

2. The axial gas holdup variation in beds of low-density particles can be regarded as negligible.

The invariant gas holdup with axial position was also observed by Smith and Ruether (1985) in their slurry bubble column system. In addition, integrating the axial solids holdups obtained from Eqs. 1 and 3 gives an overall solids mass within ±8% of the solids weight, justifying that the axial solids holdup can be determined accurately by using the conductivity probe, differential pressure measurements, and Eqs. 1 and 3.

Average gas holdup

The average gas holdup of the three-phase fluidized beds was evaluated using the quick-closing-valve technique. Figure 4 shows the variation of the average gas holdup with the superficial gas velocity for a gas-liquid system (bubble column), and fluidized beds of 4.8 vol. % of polystyrene, acrylic, and acetate particles. It is seen that the addition of solid particles to the gas-liquid system reduces the gas holdup. The overall gas holdup appears to decrease with increasing terminal velocity of the particles employed.

Axial solids holdup distribution

In a slurry bubble column system, the solids concentration can usually be well described by an exponential function of axial position. This is, however, not the case in the present system. Furthermore, there exists a constant solids concentration region near the distributor, which may result from the jetting of gas and liquid flows. Figure 5 shows the axial solids holdup distribution of polystyrene 2.0 mm particles. It is seen that at a superficial liquid velocity of 0.008 m/s, the effect of gas velocity in the range from 0.007 to 0.028 m/s on the axial solids holdup distri-

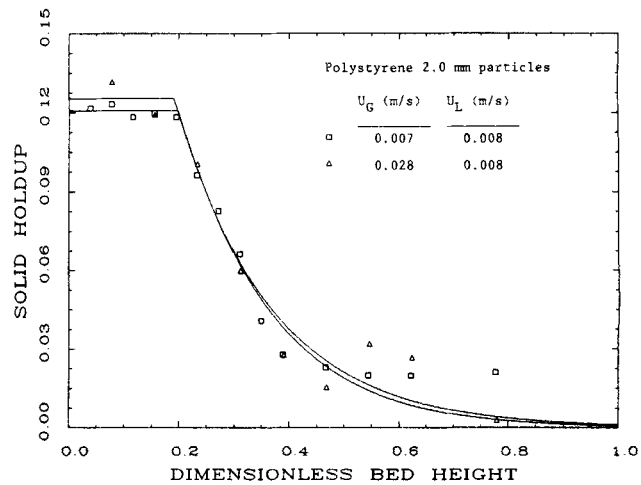

Figure 5. Effects of superficial gas velocity on axial solids holdup distribution, polystyrene particles.
Curves: results fitted by proposed model

bution is small. The small effect of gas velocity on the axial solids holdup distribution was also observed by Smith and Ruether (1985) in a slurry bubble column at gas velocities much higher than those used in this study. Figure 5 also shows that increasing gas velocity tends to slightly increase the solids concentration near the distributor region.

The bubble size distributions for beds of polystyrene particles at a superficial liquid velocity of 0.008 m/s and at superficial gas velocities from 0.007 to 0.028 m/s are shown in Figure 6. The bubbles are uniform in size in all four operating conditions. The average bubble chord lengths for superficial gas velocities of 0.007, 0.014, 0.021, and 0.028 m/s are 2.48, 3.00, 3.11, and 3.41 mm, respectively. The results clearly reflect that the operating conditions are characterized by the dispersed bubble flow regime.

The values of L_m, E_z, η, and x obtained from the parametric fitting procedure are tabulated in Table 2. As shown, L_m remains nearly constant with respect to gas velocity. The values of x obtained are mostly 0.8, and values of η do not vary significantly with gas velocity. It is noted that E_z increases significantly with increasing gas velocity, while the axial solids holdup distribution is only slightly affected by the gas velocity. This behavior can be attributed to an overall effect that at higher gas velocity more liquid is channeled through the bed from the bubble-engagement phase. Thus, the liquid flow through the particulate fluidization phase is greatly reduced, which in turn affects the solids dispersion.

Figure 7 shows the solids holdup distribution of polystyrene particles operated in a batch condition with the static height ratio of liquid to solids (H_L/H_S), or equivalently the solids concentrations, as the parameter. In batch operation, the particles are suspended purely by gas flow and there are no net flows of liquid and solids. It is noted that for all the conditions studied a uniform solids distribution in such an operation has never been reached. An increase in the solids concentration (or decrease in H_L/H_S) reduces the extent of nonuniformity of solids distribution. The values of E_z, x, and η obtained for the batch operations are also included in Table 2. For the same gas velocity, approximately the same E_z is obtained for different H_L/H_S. The circulation velocity of liquid in the particulate fluidization phase thus

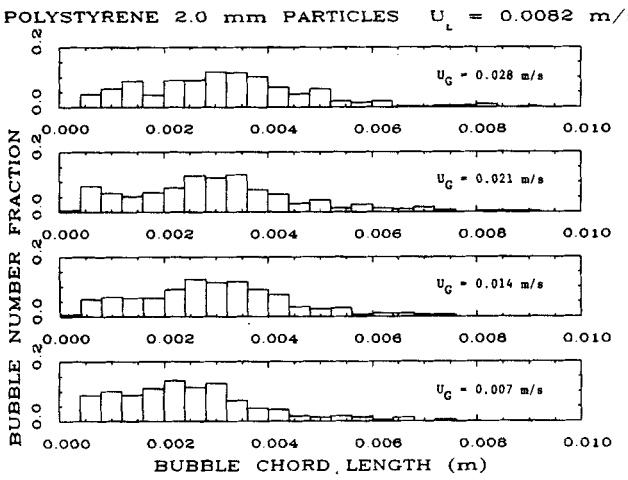

Figure 6. Bubble chord length distribution, polystyrene particles.

Table 2. Values of L_m, E_z, η, and x Obtained from Model Fitting to Experimental Data

Particle	U_L m/s	U_G m/s	Regime*	L_m m	E_z m²/s	η	x
Polystyrene	0.0082	0.0069	D	0.255	0.0106	4.61	0.8
	0.0082	0.0138	D	0.259	0.0166	4.46	0.9
	0.0082	0.0207	D	0.243	0.0363	3.89	0.8
	0.0082	0.0276	D	0.245	0.0612	3.78	0.8
H_L/H_S							
3	0.0	0.0276	D	0.117	0.0610	2.71	0.88
4	0.0	0.0276	D	0.191	0.0651	4.10	0.95
6	0.0	0.0276	D	0.174	0.0669	3.80	0.95
8	0.0	0.0276	D	0.185	0.0645	4.02	0.94
Acrylic	0.0082	0.0137	T	0.100	0.0412	4.96	0.8
	0.0082	0.0276	T	0.068	0.0599	4.08	1.3
	0.0164	0.0069	D	0.219	0.0038	2.76	0.8
	0.0164	0.0137	D	0.200	0.0066	3.97	0.8
	0.0164	0.0207	D	0.199	0.0135	4.00	0.8
	0.0164	0.0276	D	0.210	0.0260	4.05	0.8
Acetate	0.0082	0.0137	T	0.049	0.0216	4.2	0.8
	0.0082	0.0276	T	0.057	0.0262	2.6	1.3
	0.0164	0.0137	D	0.211	0.0117	3.40	0.8
	0.0164	0.0276	D	0.206	0.0299	4.96	0.8

*D, dispersed flow; T, transition flow

plays a crucial role in the uniformity of the solids distribution in the bed. A higher liquid circulation velocity is obtained for a lower total liquid height, and hence a more uniform solids distribution in the bed.

The effects of gas and liquid velocities on the axial solids holdup distribution of acrylic 1.5 mm particle are shown in Figure 8. The bed height and solids holdup determined based on the pressure gradient method are also shown in the figure. It is clear that the bed height and solids holdup thus obtained do not characterize such a system. Figure 8 also shows that decreasing liquid velocity increases the solids dispersion significantly. This is because, over the gas velocity range studied, a few regime transition from the dispersed bubble regime to the transition regime

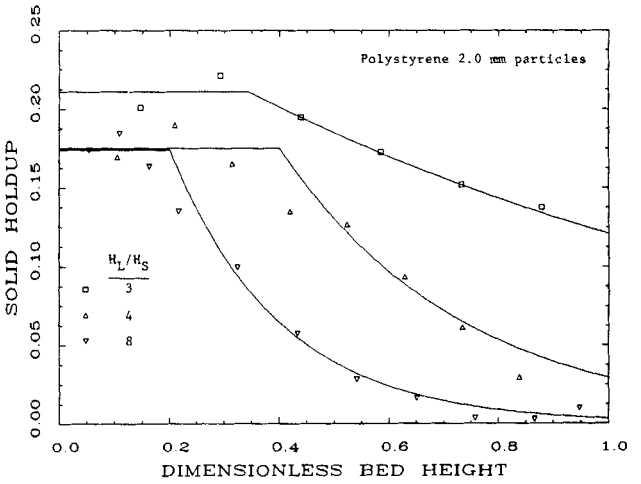

Figure 7. Axial solids holdup distribution, polystyrene particles, batch operation.

$U_L = 0$ m/s

Curves: results fitted by proposed model

between the dispersed and coalesced regimes occurs due to the liquid velocity. The bubble chord length distributions for fluidized beds of acrylic particles at various gas and liquid velocities are shown in Figure 9. At a liquid velocity of 0.016 m/s and a gas velocity of 0.014 m/s, the bubbles in the bed were observed to be ellipsoidal in shape, fairly uniform in size, and to rise without coalescence. The maximum chord length is less than 8.0 mm (or approximately 12 mm in terms of equivalent diameter) for gas velocities of both 0.014 and 0.028 m/s. On the other hand, at the lower liquid velocity (i.e., 0.008 m/s) bubbles with a chord length larger than 11 mm (the corresponding equivalent diameter being greater than 15 mm) were observed to emerge and rise in the center of the bed. The mean bubble chord lengths for all the conditions, ranging from 3.03 to 4.13 mm, do not vary considerably. Therefore, the large bubbles, although in much smaller number, are the dominating factor responsible for the solids dispersion. Increasing the gas velocity from 0.014 to 0.028 m/s increases the bubble size and the relative proportion of large bubbles, and hence an increased solids dispersion.

The results calculated based on the proposed model using the parametric values for L_m, E_z, η, and x as given in Table 2 are also shown in Figure 8. A very good agreement between the model and the experimental data is obtained. At a higher superficial liquid flow rate (in the dispersed bubble regime), L_m remains approximately constant with respect to gas velocity. At a lower liquid flow rate (in the transition regime), L_m decreases with increasing gas velocity, and the solids holdup in this region increases with gas velocity, marking a phenomenon resembling bed contraction. Under the same superficial liquid velocity, E_z increases appreciably with the superficial gas velocity. Note that the same solids axial dispersion coefficient also fits very well the axial solids holdup distribution for two overall solids concentrations (4.8 and 9.5 vol. %) operated under the same conditions and flow regime (U_G = 0.014 m/s and U_L = 0.016 m/s).

The effect of liquid velocity on the solids dispersion of acetate 1.0 mm particles, shown in Figure 10, resembles that for acrylic particles. In this case a flow regime transition is also encountered as liquid velocity is reduced from 0.016 to 0.008 m/s. At a given flow regime, the effect of gas velocity on the solids dispersion of acetate particles is found to be small.

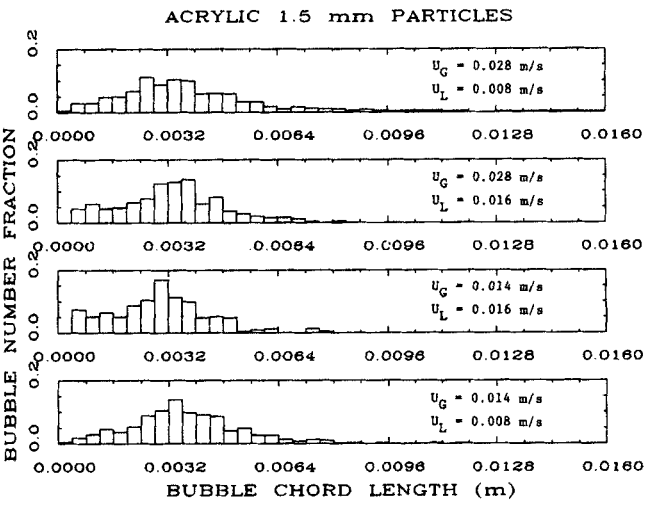

Figure 9. Bubble chord length distribution, acrylic particles.

As shown in Table 2, the values of x obtained for different particles and operating conditions lie mostly between 0.8 to 0.95, which is in reasonable agreement with that calculated based on the El-Temtamy and Epstein (1978) equation where the calculated x values vary from 0.78 to 0.92. Values of η do not vary significantly with gas velocity; neither do they vary significantly with the constraint imposed on x in the parametric estimation. The η values consistently lie between 2.0 and 5.0, which is in good agreement with the results obtained by Tsuchiya and Fan (1988), who showed that η for a spherical cap bubble rising in a liquid-solid fluidized bed varies from 2 to 6. Under the dispersed bubble regime, the values of L_m are approximately constant for all three particles. It appears that the smaller the terminal velocity of the solids, the larger the value of L_m.

E_z is a decreasing function of solids terminal velocity, as evidenced in Table 2. In the dispersed bubble regime, a correlation equation for E_z expressed as a function of the particle terminal

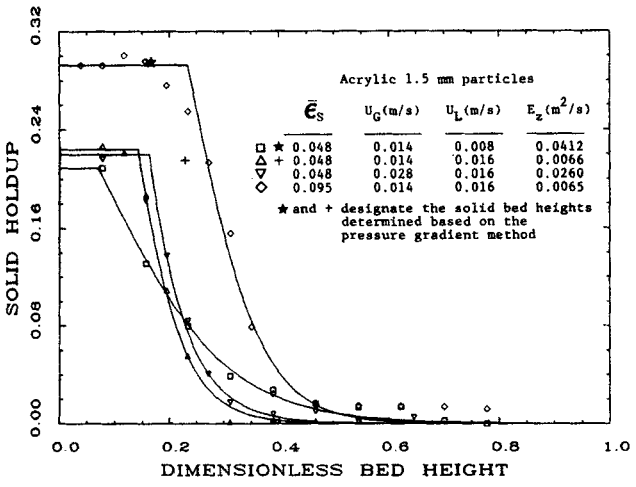

Figure 8. Axial solids holdup distribution, acrylic particles.
Curves: results fitted using proposed model

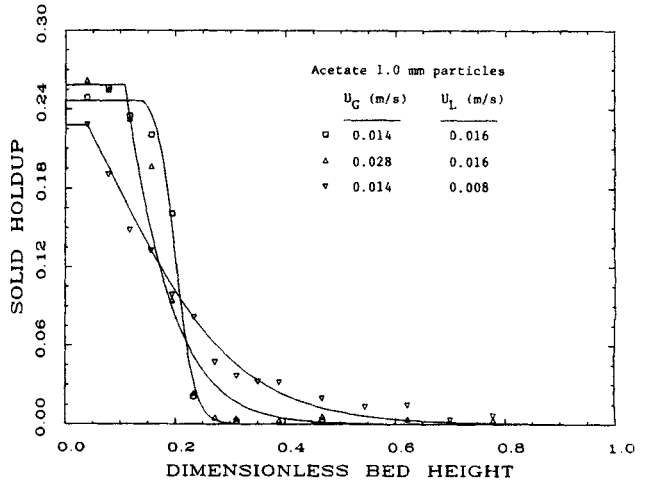

Figure 10. Axial solids holdup distribution, acetate particles.
Curves: results fitted using proposed model

velocity and the superficial gas velocity is obtained as:

$$E_z = 0.080\, U_G^{1.34} U_{t0}^{-1.22} \tag{29}$$

with a correlation coefficient of 0.976. In Eq. 29, E_z is in m^2/s, U_G and U_{t0} are in m/s. For practical purposes, a value of 3.5 and 0.8–0.9 for η and x, respectively, can be used together with Eqs. 24 to 27 and 29 to estimate the solids holdup distribution in a three-phase fluidized bed of particles with U_{t0} ranging from 0.025 to 0.055 m/s and operated in the dispersed bubble regime.

Conclusions

The solids concentration in three-phase fluidized beds containing low-density particles exhibits a significant axial variation. Utilizing an electrical conductivity probe coupled with differential pressure profile to make measurements is a viable approach for determining the axial phase holdups in such systems. For spherical particles larger than 1.5 mm, the data from the conductivity probe can be accurately related to the liquid holdup in a three-phase fluidized bed by the Buyevich (1974) equation. The Bruggeman (1935) or Maxwell (1881) equations can be used for particles smaller than 1.5 mm. The axial variation of gas holdup in this system is negligible.

In the dispersed bubble regime, gas velocity has only a slight effect on the axial solids holdup distribution. The solids dispersion increases significantly with a decrease in the liquid velocity, corresponding to a transition from the dispersed to the coalesced bubble regime. In the transition regime, the effect of gas velocity on the axial solids holdup distribution is not appreciable.

The proposed mechanistic model has the same form as the so-called dispersion-sedimentation model but offers significant physical interpretation of the model parameters. For a three-phase fluidized bed of low density and intermediate size particles under dispersed bubble regime operating conditions, the model has been demonstrated to satisfactorily account for the axial solids holdup distribution behavior.

Acknowledgment

This work was supported by National Science Foundation Grant No. CBT-8516874. W.-T. Tang was supported by the Ohio Mining and Mineral Resources Research Institute Fellowship.

Notation

A_d = effective area through which solids deentrainment flux crosses, m^2
A_e = effective area through which solids entrainment flux crosses, m^2
C_S = solids concentration; weight of solids per unit volume of both solids and liquid, kg/m^3
d_p = diameter of solid particles, m
E_z = axial solids dispersion coefficient, m^2/s
F_W = frictional force between fluids and wall, N
g = gravitational acceleration, m^2/s
H = total height of column, m
H_L = static height of liquid in batch operation, m
H_S = static solids bed height in batch operation, m
k = effective electrical conductivity of a heterogeneous system, mho
k_d = electrical conductivity of disperse phase, mho
k_c = electrical conductivity of continuous phase, mho
L_m = constant solids holdup height in a three-phase fluidized bed, m
n = Richardson-Zaki index
N_b = total number of bubbles in system
P = pressure of three-phase fluidized bed system, N/m^2
u_b = bubble rise velocity, m/s
u_L = linear liquid velocity, m/s
u_s = linear convective velocity of solids, m/s
U_G = superficial gas velocity, m/s
U_L = superficial liquid velocity, m/s
U_{mf} = minimum fluidization velocity of a liquid-solid fluidized bed, m/s
U_p = settling velocity of solids, m/s
U_{t0} = terminal velocity of a single particle in an infinite liquid medium m/s
v_d = average solids deentrainment velocity relative to bubble rise, m/s
v_e = average solids entrainment velocity relative to bubble rise, m/s
v_{Lf} = linear liquid velocity in particulate fluidization phase, m/s
v_p = linear net downward velocity of solids in particulate fluidization region, m/s
v_s = solid settling velocity relative to liquid, m/s
V_R = total volume of three-phase fluidized bed, m^3
W = total weight of solids loaded to system, kg
x = solids partition coefficient, $= \epsilon_{Se}/\epsilon_{Sf}$
z = axial coordinate, m.

Greek letters

$\alpha = k_d/k_c$
$\beta = (\alpha - 1)/(\alpha - 2)$
ϵ_d = volume fraction of dispersed phase in a heterogeneous system
ϵ_e = overall volume fraction of bubble-engagement phase
ϵ_f = overall volume fraction of particulate fluidization phase
ϵ_G = axial volume fraction of gas phase in a three-phase fluidized bed
$\bar{\epsilon}_G$ = overall volume fraction of gas phase in a three-phase fluidized bed
ϵ_L = axial volume fraction of liquid phase in a three-phase fluidized bed
ϵ_{Lf} = axial liquid volume fraction in particulate fluidization phase
ϵ_S = axial volume fraction of solids phase in a three-phase fluidized bed
$\bar{\epsilon}_S$ = overall volume fraction of solids in a three-phase fluidized bed
ϵ_{Se} = axial volume fraction of solids in bubble-engagement phase
ϵ_{Sf} = axial volume fraction in particulate fluidization phase
$\eta = \epsilon_e/\bar{\epsilon}_G$.
ρ_G = density of gas, kg/m^3
ρ_L = density of liquid, kg/m^3
ρ_S = density of solid particles, kg/m^3

Literature Cited

Begovich, J. M., and J. S. Watson, "An Electroconductivity Technique for the Measurement of Axial Variation of Holdups in Three-Phase Fluidized Beds," *AIChE J.*, **24**, 351 (1978).

Bruggeman, D. A. G., "Berechnung Verschiedener Physikalischer Konstanten von Heterogenen Substanzen," *Ann. Physik*, **24**, 636 (1935).

Brian, B. W., and P. N. Dyer, "The Effect of Gas and Liquid Velocities and Solid Size on Solid Suspension in a Three-Phase Bubble Column Reactor," *Am. Chem. Soc. Symp. Ser.*, **237**, 107 (1984).

Buyevich, Y. A., "On the Thermal Conductivity of Granular Materials," *Chem. Eng. Sci.*, **29**, 37 (1974).

Cova, D. R., "Catalyst Suspension in Gas-Agitated Tubular Reactors," *Ind. Eng. Chem. Process Des. Dev.*, **5**, 20 (1966).

Dayan, A., and S. Zalmanovich, "Axial Dispersion and Entrainment of Particles in Wakes of Bubbles," *Chem. Eng. Sci.*, **37**, 1253 (1982).

De La Rue, R. E., and C. W. Tobias, "On the Conductivity of Dispersions," *J. Electrochem. Soc.*, **106**, 827 (1959).

El-Temtamy, S. A., and N. Epstein, "Bubble Wake Solids Content in Three-Phase Fluidized Beds," *Int. J. Multiphase Flow*, **4**, 19 (1978).

———, "Simultaneous Solids Entrainment and Deentrainment above a Three-Phase Fluidized Bed," *Fluidization*, J. R. Grace, J. M. Matsen, eds., Plenum, New York, 519 (1980).

Farkas, E. J., and P. F. Leblond, "Solids Concentration Profile in the Bubble Column Slurry Reactor," *Can. J. Chem. Eng.*, **47**, 215 (1969).

Imafuku, K., T.-Y. Wang, K. Koide, and H. Kubota, "The Behavior of Suspended Solid Particles in the Bubble Column," *J. Chem. Eng. Japan*, **1**, 153 (1968).

Kato, Y., A. Nishiwaki, T. Fukuda, and S. Tanaka. "The Behavior of Suspended Solid Particles and Liquid in Bubble Columns," *J. Chem. Eng. Japan*, **5**, 112 (1972).

Kato, Y., K. Uchida, T. Kago, and S. Morooka, "Liquid Holdup and Heat Transfer Coefficient between Bed and Wall in Liquid-Solid and Gas-Liquid-Solid Fluidized Beds," *Powder Technol.*, **28**, 173 (1981).

Kato, Y., S. Morooka, T. Kago, T. Saruwatari, and S.-Z. Yang, "Axial Holdup Distributions of Gas and Solid Particles in Three-Phase Fluidized Bed for Gas-Liquid (Slurry)-Solid System," *J. Chem. Eng. Japan*, **18**, 308 (1985).

Kitano, K., and L.-S. Fan, "Near-Wake Structure of a Single Gas Bubble in a Two-Dimensional Liquid-Solid Fluidized Bed: Solid Holdup," *Chem. Eng. Sci.*, **43**, 1355 (1988).

Kojima, H., and K. Asano, "Hydrodynamic Characteristics of a Suspension-Bubble Column," *Int. Chem. Eng.*, **21**, 473 (1981).

Matsuura, A., and L.-S. Fan, "Distribution of Bubble Properties in a Gas-Liquid-Solid Fluidized Bed," *AIChE J.*, **30**, 894 (1984).

Maxwell, J. C., *A Treatise on Electricity and Magnetism*, 2nd ed., **I**, 435 (1881).

Meredith, R. E., and C. W. Tobias, "Conductivities in Heterogeneous Systems," *Advances in Electrochemistry and Electrochemical Engineering*, **2**, Interscience, New York, 15 (1962).

Nasr-El-Din, H., C. A. Shook, and J. Colwell, "A Conductivity Probe for Measuring Local Concentrations in Slurry Systems," *Int. J. Multiphase Flow*, **13**, 365 (1987).

Page, R. E., and D. Harrison, "Particle Entrainment from a Three-Phase Fluidized Bed," *Fluidization and Its Applications*, Angelino et al., eds., 393 (1974).

Richardson, J. F., and W. N. Zaki, "Sedimentation and Fluidization: I," *Trans. Inst. Chem. Engrs.*, **32**, 35 (1954).

Smith, D. N., and J. A. Ruether, "Dispersed Solid Dynamics in a Slurry Bubble Column," *Chem. Eng. Sci.*, **40**, 741 (1985).

Tsuchiya, K., and L.-S. Fan, "Near-Wake Structure of a Single Bubble in a Two-Dimensional Liquid-Solid Fluidized Bed: Vortex Shedding and Wake Size Variation," *Chem. Eng. Sci.*, **43**, 1167 (1988).

Turi, E., and K. M. Ng, "Axial Distribution of Solid Particles in Bubble Column Slurry Reactors in the Bubble Flow Regime," *Chem. Eng. Commun.*, **46**, 323 (1986).

Turner, J. C. R., "Two-Phase Conductivity: The Electrical Conductance of Liquid-Fluidized Beds of Spheres," *Chem. Eng. Sci.*, **31**, 487 (1976).

Ueyama, K., N. Tamura, and S. Furusaki, "Distribution of Holdup of Particles in a Three-Phase Fluidized Bed," *Fluidization '85 Science and Technology*, Kwauk et al., eds., 274 (1985).

Manuscript received Apr. 29, 1988, and revision received Sept. 8, 1988.